Short Papers

Mobility Augmentation of Conventional Wheeled Bases for Omnidirectional Motion

Myung-Jin Jung and Jong-Hwan Kim

***Abstract*—This paper presents the mobility augmentation method to provide omnidirectional mobility to nonomnidirectional wheeled bases. First, the kinematic model of a nonomnidirectional wheeled base and a link combined by an extra revolute/prismatic joint to the base is derived in a matrix-vector form. Then it is shown that, if the kinematic model satisfies some structural conditions, the link motion can be omnidirectional. The structural conditions for omnidirectional motion are derived and several examples are provided to demonstrate the method.**

***Index Terms*—Mobility augmentation, omnidirectional motion, structural conditions.**

I. Introduction

Omnidirectional mobile robots can move in any direction in the configuration space formed by the basis representing the robot position (x, y) and orientation θ with respect to a global coordinate frame. If the wheels of the robot need to be reoriented, then it is nonholonomic; otherwise, it is holonomic. In this paper, only holonomic omnidirectional robots are considered. Since there is no nonholonomic constraint on the robot motion, such robots have the full degree of mobility [1]. The most well-known mechanisms are those using omnidirectional wheels such as ballwheels or Mecanum wheels [2], [8], [10]. These omnidirectional wheel mechanisms are perfect in principle: the symmetric wheel arrangement distributes the load equally to each wheel. However, in practice, such omnidirectional wheels have some demerits compared with tirewheels. The ballwheel often slips in the dusty environment because of the rolling contact with the actuator and the ground. The Mecanum wheel has discontinuous contact with the ground, resulting in vibration or a larger kinematic modeling error. There is another holonomic omnidirectional mechanism which uses conventional tirewheels [4], [9]. In this mechanism, each wheel module uses two motors to accomplish omnidirectional motion. Since at least two wheel modules are required for omnidirectional motion of the robot, the mechanism needs at least four actuators. Although a tirewheel exhibits better traction and accuracy on the floor, the four-actuator structure results in an over-constraint problem among the actuators, causing the tire or the robot to be temporarily deformed or slip during the transient period and thus incurs damages or kinematic modeling errors.

Several attempts have been made to increase the traction of ballwheels, reduce the discontinuity gap of Mecanum wheels, and minimize the effects of the over-constraint of tirewheels [3], [7], [11]. As a different approach, a mechanism that did not use conventional omnidirectional wheels was proposed in [5] and [6]. Since the omnidirectional motion was produced by a mobile base with the degree of mobility less than three and a revolute joint, such a structure, in this paper, is called a nonconventional omnidirectional wheeled mechanism. This paper presents the mobility augmentation method to construct nonconventional omnidirectional wheeled robots with an extra revolute or prismatic joint. First, the kinematic model of a nonomnidirectional wheeled base and a link combined by an extra revolute/prismatic joint to the base is derived. Then structural conditions that the kinematic model must satisfy to generate omnidirectional motion are derived. Nonconventional omnidirectional robots, designed by applying the structural conditions, do not suffer from an over-constraint problem, which is typical in conventional tirewheeled mechanisms.

In Section II, the motion constraints and the degree of mobility of wheeled mobile robots are revisited. In Section III, the kinematic model of conventional wheeled bases combined with a revolute/prismatic joint is obtained and the structural conditions that the kinematic model must satisfy for omnidirectional motion are derived. Section IV provides some nonconventional omnidirectional mechanisms designed by applying the structural conditions. Among the example mechanisms, the most practical case is chosen to develop OmniKity-III. In Section V, OmniKity-III, a nonconventional omnidirectional wheeled robot, is described with the kinematic model and its fault-tolerance property. Concluding remarks follow in Section VI.

II. Robot Motion Constraints

In Fig. 1(a), let $\Sigma_{\mathbf{R}}$, $\Sigma_{\mathbf{r}}$, and $\Sigma_{\mathbf{F}}$ be the global coordinate frame, the robot coordinate frame, and the robot instantaneously coincident frame, respectively. Let ${}^{\mathbf{R}}\mathbf{x} = [\,x \quad y\,]^T$ denote the robot position and ${}^{\mathbf{R}}\mathbf{p} = [\,x \quad y \quad \theta\,]^T$ denote the robot posture in $\Sigma_{\mathbf{R}}$. We define the rotation matrix $R(\theta)$ as

$$R(\theta) \triangleq \begin{bmatrix} \cos\theta & -\sin\theta & 0 \\ \sin\theta & \cos\theta & 0 \\ 0 & 0 & 1 \end{bmatrix}. \tag{1}$$

Then the robot motion ${}^{\mathbf{R}}\dot{\mathbf{p}} = [\,\dot{x} \quad \dot{y} \quad \dot{\theta}\,]^T$ is constrained by the wheels as follows [1]:

1) Offset-centered orientable wheel (Fig. 1(b))
   - Along the wheel plane

$$[\,-\sin(\alpha_{oc}+\beta_{oc}) \quad \cos(\alpha_{oc}+\beta_{oc}) \quad l_{oc}\cos\beta_{oc}\,]\,R^{-1}(\theta)\,{}^{\mathbf{R}}\dot{\mathbf{p}} + r_{oc}\dot{\phi}_{oc} = 0.$$

   - Along the wheel axis

$$[\,\cos(\alpha_{oc}+\beta_{oc}) \quad \sin(\alpha_{oc}+\beta_{oc}) \quad d_{oc}+l_{oc}\sin\beta_{oc}\,] \times R^{-1}(\theta)\,{}^{\mathbf{R}}\dot{\mathbf{p}} + d_{oc}\dot{\beta}_{oc} = 0.$$

2) Centered orientable or fixed wheel [Fig. 1(c)]
   - Along the wheel plane

$$[\,-\sin(\alpha_f+\beta_f) \quad \cos(\alpha_f+\beta_f) \quad l_f\cos\beta_f\,]\,R^{-1}(\theta)\,{}^{\mathbf{R}}\dot{\mathbf{p}} + r_f\dot{\phi}_f = 0.$$

   - Along the wheel axis

$$[\,\cos(\alpha_f+\beta_f) \quad \sin(\alpha_f+\beta_f) \quad l_f\sin\beta_f\,]\,R^{-1}(\theta)\,{}^{\mathbf{R}}\dot{\mathbf{p}} = 0.$$

Manuscript received September 6, 2001. This paper was recommended for publication by Associate Editor Y. Xu and Editor I. Walker upon evaluation of the reviewers' comments. This work was supported in part by the Korea Ministry of Science and Technology (MOST) under Grant 98-N9-01-01-A and in part by the HWRS ERC center at the Korea Advanced Institute of Science and Technology (KAIST).

The authors are with the Department of Electrical Engineering and Computer Science, KAIST, Korea (e-mail: {mjjung; johkim}@vivaldi.kaist.ac.kr).

Publisher Item Identifier S 1042-296X(02)01811-6.

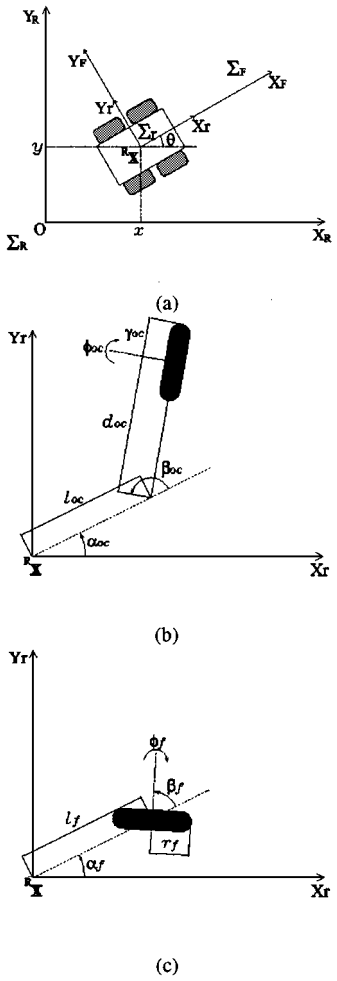

Fig. 1. (a) Coordinate systems. (b) Wheel configuration parameters of offset-centered orientable wheel w.r.t. the robot frame. (c) Wheel configuration parameters of fixed/centered orientable wheel w.r.t. the robot frame.

If there are N_{oc} offset-centered orientable wheels and N_f fixed or centered orientable wheels, all the constraints can be arranged in a matrix-vector form as follows:

$$\begin{bmatrix} J_1(\beta_{oc},\beta_f) \\ C_{1oc}(\beta_{oc}) \\ C_{1f}(\beta_f) \end{bmatrix} R^{-1}(\theta)\,{}^{\mathbf{R}}\dot{\mathbf{p}} + \begin{bmatrix} J_2 & \mathbf{0} \\ \mathbf{0} & C_{2oc} \\ \mathbf{0} & \mathbf{0} \end{bmatrix} \begin{bmatrix} \dot{\phi} \\ \dot{\beta} \end{bmatrix} = \mathbf{0} \tag{2}$$

where $[\,\dot{\phi}^T \quad \dot{\beta}^T\,]^T$ is a vector form of N_{oc} $\dot{\phi}_{oc}$'s, N_f $\dot{\phi}_f$'s and N_{oc} $\dot{\beta}_{oc}$'s. Coefficient matrices $J_1(\beta_{oc},\beta_f)$, J_2, $C_{1oc}(\beta_{oc})$, C_{2oc}, and $C_{1f}(\beta_f)$ are an $(N_{oc}+N_f)\times 3$ matrix, an $(N_{oc}+N_f)\times(N_{oc}+N_f)$ matrix, an $N_{oc}\times 3$ matrix, an $N_{oc}\times N_{oc}$ matrix, and an $N_f\times 3$ matrix, respectively, and are readily derived from the constraints.

Among the constraints, Campion and Bastin [1] focused on the following condition:

$$C_{1f}R^{-1}(\theta)\,{}^{\mathbf{R}}\dot{\mathbf{p}} = \mathbf{0}. \tag{3}$$

By (3), $R^{-1}(\theta)\,{}^{\mathbf{R}}\dot{\mathbf{p}}$, the base motion with respect to $\mathbf{\Sigma_F}$, is restricted to the null space of C_{1f}. Campion and Bastin defined the degree of mobility δ_m of conventional wheeled bases as

$$\delta_m = 3 - \mathtt{rank}\,(C_{1f})\,. \tag{4}$$

The attempt made in this paper is to attach a link to the wheeled base with a revolute/prismatic joint so that the link motion is not restricted to any null space whereby the full mobility ($\delta_m = 3$) is achieved.

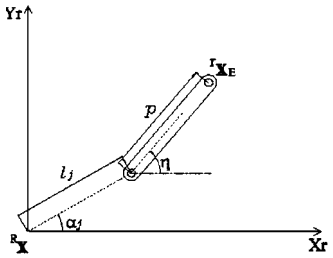

Fig. 2. Joint configuration parameters w.r.t. the robot frame.

III. Mobility Augmentation

In Fig. 2, ${}^{\mathbf{r}}\mathbf{x_E}$ represents the location of a link in $\mathbf{\Sigma_r}$ attached by either a prismatic or a revolute joint to the base. The link posture ${}^{\mathbf{r}}\mathbf{p_E}$ in $\mathbf{\Sigma_r}$ is given by

$${}^{\mathbf{r}}\mathbf{p_E} = \begin{bmatrix} l_j\cos\alpha_j + p\cos\eta \\ l_j\sin\alpha_j + p\sin\eta \\ \eta \end{bmatrix} \tag{5}$$

where l_j and α_j represent the joint location and p and η represent the joint axis. If the joint is prismatic, p is the control variable and η is fixed. If the joint is revolute, p is fixed and η is the control variable.

Then the link posture ${}^{\mathbf{R}}\mathbf{p_E} = [\,x_E \quad y_E \quad \theta_E\,]^T$ and its motion with respect to $\Sigma_{\mathbf{R}}$ are given by

$${}^{\mathbf{R}}\mathbf{p_E} = {}^{\mathbf{R}}\mathbf{p} + R(\theta)\,{}^{\mathbf{r}}\mathbf{p_E} \tag{6}$$

$${}^{\mathbf{R}}\dot{\mathbf{p}}_{\mathbf{E}} = {}^{\mathbf{R}}\dot{\mathbf{p}} + \dot{R}(\theta)\,{}^{\mathbf{r}}\mathbf{p_E} + R(\theta)\,{}^{\mathbf{r}}\dot{\mathbf{p}}_{\mathbf{E}} \tag{7}$$

respectively.

Let's define ${}^{\mathbf{F}}\mathbf{v_E} = [\,{}^{\mathbf{F}}v_{xE} \quad {}^{\mathbf{F}}v_{yE} \quad {}^{\mathbf{F}}v_{\theta E}\,]^T \triangleq R^{-1}(\theta)\,{}^{\mathbf{R}}\dot{\mathbf{p}}_{\mathbf{E}}$ which represents the link motion with respect to $\Sigma_{\mathbf{F}}$. In the following, the motion constraints are represented in terms of ${}^{\mathbf{F}}\mathbf{v_E}$ since the affine transformation ${}^{\mathbf{F}}\mathbf{v_E} = R^{-1}(\theta)\,{}^{\mathbf{R}}\dot{\mathbf{p}}_{\mathbf{E}}$ does not change the constraint properties of ${}^{\mathbf{R}}\dot{\mathbf{p}}_{\mathbf{E}}$. From (7), ${}^{\mathbf{F}}\mathbf{v_E}$ is obtained as

$${}^{\mathbf{F}}\mathbf{v_E} = R^{-1}(\theta)\,{}^{\mathbf{R}}\dot{\mathbf{p}} + R^{-1}(\theta)\dot{R}(\theta)\,{}^{\mathbf{r}}\mathbf{p_E} + {}^{\mathbf{r}}\dot{\mathbf{p}}_{\mathbf{E}} \tag{8}$$

$$= R^{-1}(\theta)\,{}^{\mathbf{R}}\dot{\mathbf{p}} + \begin{bmatrix} -l_j\sin\alpha_j - p\sin\eta \\ l_j\cos\alpha_j + p\cos\eta \\ 0 \end{bmatrix}\dot{\theta} + {}^{\mathbf{r}}\dot{\mathbf{p}}_{\mathbf{E}}. \tag{9}$$

By substituting $R^{-1}(\theta)\,{}^{\mathbf{R}}\dot{\mathbf{p}}$ of (9) into (2), the constraint equations become

$$\begin{bmatrix} J_1 \\ C_{1oc} \\ C_{1f} \end{bmatrix} \left({}^{\mathbf{F}}\mathbf{v_E} + \begin{bmatrix} l_j\sin\alpha_j + p\sin\eta \\ -l_j\cos\alpha_j - p\cos\eta \\ 0 \end{bmatrix}\dot{\theta} - {}^{\mathbf{r}}\dot{\mathbf{p}}_{\mathbf{E}} \right) + \begin{bmatrix} J_2 & \mathbf{0} \\ \mathbf{0} & C_{2oc} \\ \mathbf{0} & \mathbf{0} \end{bmatrix} \begin{bmatrix} \dot{\phi} \\ \dot{\beta} \end{bmatrix} = \mathbf{0}. \tag{10}$$

Let

$$A_o \triangleq \begin{bmatrix} J_1 \\ C_{1oc} \\ C_{1f} \end{bmatrix}_{2(N_{oc}+N_f)\times 3} = [\,\mathbf{a_1} \quad \mathbf{a_2} \quad \mathbf{a_3}\,] \tag{11}$$

$$B_o \triangleq \begin{bmatrix} -J_2 & \mathbf{0} \\ \mathbf{0} & -C_{2oc} \\ \mathbf{0} & \mathbf{0} \end{bmatrix}_{2(N_{oc}+N_f)\times(2N_{oc}+N_f)} \tag{12}$$

where $\mathbf{a_i}(i = 1,2,3)$ are the column vectors of A_o. Next we examine the cases when the joint is prismatic or revolute.

A. Prismatic Joint

If the joint is prismatic, we get

$$ {}^{\mathbf{r}}\dot{\mathbf{p}}_{\mathbf{E}} = \begin{bmatrix} \cos\eta \\ \sin\eta \\ 0 \end{bmatrix} \dot{p} \tag{13} $$

and ${}^{\mathbf{F}}v_{\theta E} = \dot{\theta}$. Therefore, (10) is rearranged as

$$ [\,\mathbf{a_1} \quad \mathbf{a_2} \quad \mathbf{a}_3'\,]\,{}^{\mathbf{F}}\mathbf{v}_{\mathbf{E}} = [\,B_o \quad \cos\eta\mathbf{a_1} + \sin\eta\mathbf{a_2}\,] \begin{bmatrix} \dot{\phi} \\ \dot{\beta} \\ \dot{p} \end{bmatrix} \tag{14} $$

where

$$ \mathbf{a}_3' = (l_j \sin\alpha_j + p\sin\eta)\,\mathbf{a_1} - (l_j\cos\alpha_j + p\cos\eta)\,\mathbf{a_2} + \mathbf{a_3}. \tag{15} $$

B. Revolute Joint

If the joint is revolute, we get

$$ {}^{\mathbf{r}}\dot{\mathbf{p}}_{\mathbf{E}} = \begin{bmatrix} -p\sin\eta \\ p\cos\eta \\ 1 \end{bmatrix} \dot{\eta} \tag{16} $$

and ${}^{\mathbf{F}}v_{\theta E} = \dot{\theta} + \dot{\eta}$. Therefore, (10) is rearranged as

$$ \begin{aligned} &[\,\mathbf{a_1} \quad \mathbf{a_2} \quad \mathbf{a}_3'\,]\,{}^{\mathbf{F}}\mathbf{v}_{\mathbf{E}} \\ &\qquad = [\,B_o \quad l_j\sin\alpha_j\mathbf{a_1} - l_j\cos\alpha_j\mathbf{a_2} + \mathbf{a_3}\,] \begin{bmatrix} \dot{\phi} \\ \dot{\beta} \\ \dot{p} \end{bmatrix} \end{aligned} \tag{17} $$

where $\mathbf{a}_3'$ is the same as that in (15).

The constraint (14) and (17) can be written in the following form:

$$ A\,{}^{\mathbf{F}}\mathbf{v}_{\mathbf{E}} = B\mathbf{u}. \tag{18} $$

The objective is to steer the output ${}^{\mathbf{F}}\mathbf{v}_{\mathbf{E}}$ in the omnidirectional manner with the input $\mathbf{u}$. In the following, we derive conditions of A and B to achieve this.

C. Omnidirectional Steering

Theorem 1: ${}^{\mathbf{F}}\mathbf{v}_{\mathbf{E}}$ $(\in \mathbf{R^3})$ of systems (14) and (17) which are represented in the the following matrix-vector form:

$$ A\,{}^{\mathbf{F}}\mathbf{v}_{\mathbf{E}} = B\mathbf{u} \tag{19} $$

can be steered in the omnidirectional manner with the input $\mathbf{u}$ if:

1) rank B = rank $[BA]$;
2) rank $A = 3$.

Proof : First, let us assume B has full rank (rank $B = \dim \mathbf{u}$). If rank $B < \dim \mathbf{u}$, B and $\mathbf{u}$ can be rearranged in such a way that

$$ B\mathbf{u} = [\,B_I \quad B_D\,] \begin{bmatrix} \mathbf{u_I} \\ \mathbf{u_D} \end{bmatrix} $$

where rank B_I = rank B and all the columns of B_I are linearly independent of one another. By letting $\mathbf{u_D} = \mathbf{0}$, (19) is rewritten as

$$ A\,{}^{\mathbf{F}}\mathbf{v}_{\mathbf{E}} = B_I\mathbf{u_I} \tag{20} $$

where B_I is full rank. Therefore, without losing generality, we can assume the matrix B in (19) is full rank.

If the first condition of the theorem is satisfied, the right-hand side of (19) can be represented as

$$ \begin{aligned} B\mathbf{u} &= [\,A \quad A_C\,] \begin{bmatrix} \mathbf{u_A} \\ \mathbf{u_C} \end{bmatrix} \\ &= A\mathbf{u_A} + A_C\mathbf{u_C} \end{aligned} \tag{21} $$

where A_C has maximal rank (rank A_C = rank B − rank A). With such A_C and the full rank condition of B, $[\,(\mathbf{u_A})^T \quad (\mathbf{u_C})^T\,]^T$ has the equivalence relation with $\mathbf{u}$ in such a way that

$$ \begin{bmatrix} \mathbf{u_A} \\ \mathbf{u_C} \end{bmatrix} = (D^TD)^{-1}D^TB\mathbf{u} \quad \text{or} \quad \mathbf{u} = (B^TB)^{-1}B^TD \begin{bmatrix} \mathbf{u_A} \\ \mathbf{u_C} \end{bmatrix} \tag{22} $$

where $D = [\,A \quad A_C\,]$. Therefore, $[\,(\mathbf{u_A})^T \quad (\mathbf{u_C})^T\,]^T$ can be regarded as the equivalence of the unconstrained input $\mathbf{u}$.

For (19) and (21) to be consistent, $\mathbf{u_C}$ should be such that $A_C\mathbf{u_C} = \mathbf{0}$. Then

$$ A\,{}^{\mathbf{F}}\mathbf{v}_{\mathbf{E}} = A\mathbf{u_A} \tag{23} $$

or

$$ A({}^{\mathbf{F}}\mathbf{v}_{\mathbf{E}} - \mathbf{u_A}) = \mathbf{0}. \tag{24} $$

Since rank $A = 3 = \dim({}^{\mathbf{F}}\mathbf{v}_{\mathbf{E}})$, Nullity $(A) = 0$, hence ${}^{\mathbf{F}}\mathbf{v}_{\mathbf{E}} = \mathbf{u_A}$. Because $\mathbf{u_A}$ is unconstrained, ${}^{\mathbf{F}}\mathbf{v}_{\mathbf{E}}$ can be steered in the omnidirectional manner with $\mathbf{u_A}$. □

Remark 1: To obtain the link motion w.r.t. $\Sigma_{\mathbf{R}}$, which is given by ${}^{\mathbf{R}}\dot{\mathbf{p}}_{\mathbf{E}} = R(\theta)\,{}^{\mathbf{F}}\mathbf{v}_{\mathbf{E}}$, the motion equation of θ is needed. It is given by

$$ \dot{\theta} = \begin{cases} {}^{\mathbf{F}}v_{\theta E}, & \text{if the joint is prismatic,} \\ {}^{\mathbf{F}}v_{\theta E} - \dot{\eta}, & \text{if the joint is revolute.} \end{cases} \tag{25} $$

Remark 2: All conventional omnidirectional wheeled mobile bases can be represented by (19) and satisfy the conditions of **Theorem 1**.

Remark 3: For the systems of (14) and (17), rank $A_C = \dim(\mathbf{u_C})$ because the number of rows of A_C is $2(N_F + N_{oc})$ while the number of columns is less than $N_F + 2N_{oc} + 1$. Therefore, $A_C\mathbf{u_C} = \mathbf{0}$ implies $\mathbf{u_C} = \mathbf{0}$. This condition states that if there are more degrees of freedom in joint motion than those in robot motion, the extra degrees of joint motion are constrained in the form of $\mathbf{u_C} = \mathbf{0}$. By inspecting this joint motion constraint, the minimum set of actuated joints for maneuvering omnidirectional motion without singular configurations can be decided. If a joint motion can always be represented by the other joint motions, the joint can be passive to avoid the over-constraint problem without affecting omnidirectional mobility.

In what follows, several structures with a conventional wheeled base combined with a prismatic/revolute joint are examined to see if they can produce omnidirectional motion using **Theorem 1**. Then, by applying the condition $\mathbf{u_C} = \mathbf{0}$, the minimum set of actuated joints will be decided.

IV. Omnidirectional Motion by a Wheeled Base With $\delta_m = 2$ and a Prismatic/Revolute Joint: Case Studies

In this section, several wheeled bases with the degree of mobility equal two are provided to demonstrate the mobility augmentation method by using the structural conditions of **Theorem 1**. Using the conditions, the positions of the wheels and the joint are decided to generate omnidirectional motion of the link. Then the minimum actuated joints for maneuvering omnidirectional motion without singular configurations will also be decided.

1) Case 1: Base With a Fixed and an Offset-Centered Orientable Wheel + a Prismatic Joint: Fig. 3 shows the case where two wheels are attached to the base, one fixed and one offset-centered orientable

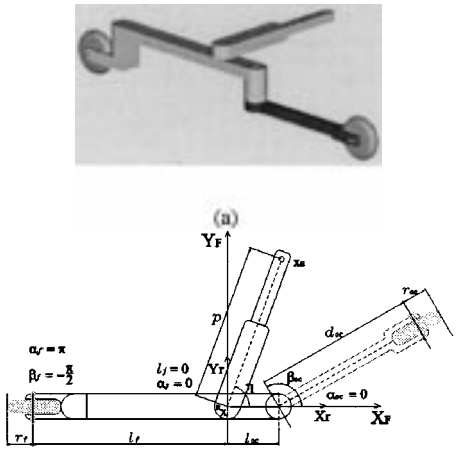

Fig. 3. Case 1. (a) 3-D view. (b) Kinematic parameters.

wheel. The link is connected to the base by a prismatic joint. The base motion ${}^{\mathbf{R}}\dot{\mathbf{p}}$ is, by the wheels, constrained to

$$\begin{bmatrix} -1 & 0 & 0 \\ -\sin\beta_{oc} & \cos\beta_{oc} & l_{oc}\cos\beta_{oc} \\ \cos\beta_{oc} & \sin\beta_{oc} & d_{oc}+l_{oc}\sin\beta_{oc} \\ 0 & 1 & l-l_f \end{bmatrix} R^{-1}(\theta)\,{}^{\mathbf{R}}\dot{\mathbf{p}} + \begin{bmatrix} r_f & 0 & 0 \\ 0 & r_{oc} & 0 \\ 0 & 0 & d_{oc} \\ 0 & 0 & 0 \end{bmatrix} \begin{bmatrix} \dot{\phi}_f \\ \dot{\phi}_{oc} \\ \dot{\beta}_{oc} \end{bmatrix} = \mathbf{0}. \quad (26)$$

Then, from (14), ${}^{\mathbf{F}}\mathbf{v_E}$ is constrained to (27), shown at the bottom of the page. To meet the conditions of **Theorem 1**,

- $\sin\eta \neq 0$;
- $d_{oc}^2 + (l_f + l_{oc})^2 + 2d_{oc}(l_f + l_{oc})\sin\beta_{oc} \neq 0$.

If $\sin\eta = 0$, the link motion contributes only along the $X_{\mathbf{F}}$ axis, hence the motion along the $Y_{\mathbf{F}}$ axis is not independently controllable. The second condition means the ground contact points of the two wheels must not coincide. To meet this condition, $d_{oc} \neq l_f + l_{oc}$. If both conditions are satisfied, ${}^{\mathbf{F}}\mathbf{v_E}$, hence ${}^{\mathbf{R}}\dot{\mathbf{p}}_{\mathbf{E}}$ can be controlled omnidirectionally as long as the input variables $\dot{\phi}_f$, $\dot{\phi}_{oc}$, $\dot{\beta}_{oc}$, and $\dot{p}$ are not stuck by the joint limits. The former three variables are rotational motions and such a situation can be avoided. But $\dot{p}$ is the prismatic joint velocity and it becomes stuck when the joint is fully expanded or shrunk. So even though omnidirectional motion can be achieved by attaching a prismatic joint, it is very limited within the prismatic joint work range. This is the drawback of using a prismatic joint. To overcome this, a revolute joint is used for omnidirectional motion in Cases 2 and 3.

To find the minimum set of actuated joints, the right-hand side of (27), shown at the bottom of the page, is rewritten as

$$[\,B_o \quad \cos\eta\mathbf{a_1} + \sin\eta\mathbf{a_2}\,] \begin{bmatrix} \dot{\phi}_f \\ \dot{\phi}_{oc} \\ \dot{\beta}_{oc} \\ \dot{p} \end{bmatrix} = [\,A \quad A_C\,] \begin{bmatrix} \mathbf{u_A} \\ \mathbf{u_C} \end{bmatrix}. \quad (28)$$

For simplification, let $l_{oc} = l_f = l$, $d_{oc} = d$, $r_f = r_{oc} = r$, $\beta_{oc} = \beta$, and $\eta = \pi/2$. Using A_C shown at the bottom of the page, $\mathbf{u_C}$ is found to be

$$\begin{aligned} \mathbf{u_C} = &-\frac{r(2l + d\sin\beta)}{d^2 + 4l^2 + 4dl\sin\beta}\dot{\phi}_f + \frac{r(d + 2l\sin\beta)}{d^2 + 4l^2 + 4dl\sin\beta}\dot{\phi}_{oc} \\ &- \frac{2dl\cos\beta}{d^2 + 4l^2 + 4dl\sin\beta}\dot{\beta} \\ = &0. \end{aligned} \quad (29)$$

Since $d^2 + 4l^2 + 4dl\sin\beta \neq 0$, the constraint among the input variables is represented as

$$-r(2l + d\sin\beta)\dot{\phi}_f + r(d + 2l\sin\beta)\dot{\phi}_{oc} - 2dl\cos\beta\dot{\beta} = 0. \quad (30)$$

In practical implementations, $d < 2l$ or $d > 2l$, hence either $\dot{\phi}_f$ or $\dot{\phi}_{oc}$ can be removed from the actuated joints set. Therefore, among the four input variables, $\{\dot{\phi}_f, \dot{\beta}_{oc}, \dot{p}\}$, or $\{\dot{\phi}_{oc}, \dot{\beta}_{oc}, \dot{p}\}$ represents the minimum actuated joints set.

2) Case 2: Base With a Fixed and an Offset-Centered Orientable Wheel + a Revolute Joint: Fig. 4 shows the case where two wheels are attached to the base, one fixed and one offset-centered orientable wheel, as in Case 1. The link is connected through a revolute joint. The link position is the same as the wheeled base position. The base motion ${}^{\mathbf{R}}\dot{\mathbf{p}}$ is, by the wheels, constrained to

$$\begin{bmatrix} -1 & 0 & 0 \\ -\sin\beta_{oc} & \cos\beta_{oc} & l_{oc}\cos\beta_{oc} \\ \cos\beta_{oc} & \sin\beta_{oc} & d_{oc}+l_{oc}\sin\beta_{oc} \\ 0 & 1 & -l_f \end{bmatrix} R^{-1}(\theta)\,{}^{\mathbf{R}}\dot{\mathbf{p}} + \begin{bmatrix} r_f & 0 & 0 \\ 0 & r_{oc} & 0 \\ 0 & 0 & d_{oc} \\ 0 & 0 & 0 \end{bmatrix} \begin{bmatrix} \dot{\phi}_f \\ \dot{\phi}_{oc} \\ \dot{\beta}_{oc} \end{bmatrix} = \mathbf{0}. \quad (31)$$

Then ${}^{\mathbf{F}}\mathbf{v_E}$ is constrained to

$$\begin{bmatrix} -1 & 0 & 0 \\ -\sin\beta_{oc} & \cos\beta_{oc} & l_{oc}\cos\beta_{oc} \\ \cos\beta_{oc} & \sin\beta_{oc} & d_{oc}+l_{oc}\sin\beta_{oc} \\ 0 & 1 & -l_f \end{bmatrix} {}^{\mathbf{F}}\mathbf{v_E} = [\,B_o \quad \mathbf{a_3}\,] \begin{bmatrix} \dot{\phi}_f \\ \dot{\phi}_{oc} \\ \dot{\beta}_{oc} \\ \dot{\eta} \end{bmatrix}. \quad (32)$$

$$\begin{bmatrix} -1 & 0 & -p\sin\eta \\ -\sin\beta_{oc} & \cos\beta_{oc} & -p\cos(\eta-\beta_{oc}) + l_{oc}\cos\beta_{oc} \\ \cos\beta_{oc} & \sin\beta_{oc} & p\sin(\eta-\beta_{oc}) + d_{oc} + l_{oc}\sin\beta_{oc} \\ 0 & 1 & -p\cos\eta - l_f \end{bmatrix} {}^{\mathbf{F}}\mathbf{v_E} = [\,B_o \quad \cos\eta\mathbf{a_1} + \sin\eta\mathbf{a_2}\,] \begin{bmatrix} \dot{\phi}_f \\ \dot{\phi}_{oc} \\ \dot{\beta}_{oc} \\ \dot{p} \end{bmatrix} \quad (27)$$

$$A_C = \begin{bmatrix} l + \left(\frac{d}{2}\right)\sin\beta & -\left(\frac{d}{2}\right) - l\sin\beta & l\cos\beta & \left(\frac{d}{2}\right)\cos\beta \end{bmatrix}^T$$

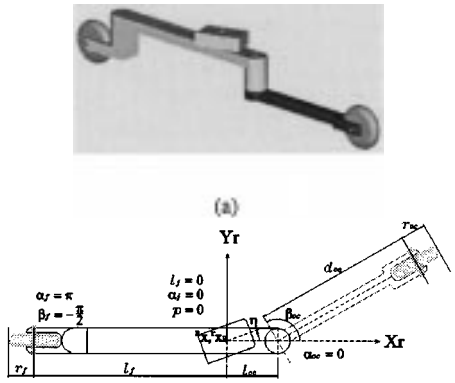

Fig. 4. Case 2. (a) 3-D view. (b) Kinematic parameters.

To meet the conditions of **Theorem 1**

- $l_f \neq 0$;
- $d_{oc}^2 + (l_f + l_{oc})^2 + 2d_{oc}(l_f + l_{oc}) \sin\beta_{oc} \neq 0$.

The first condition implies that the link position ${}^{\mathbf{R}}\mathbf{x_E}$ should not lie on the ground contact point of the fixed wheel. The second condition is the same as that of Case 1. Unlike the prismatic joint case, all the input variables are rotational motions and can avoid mechanical joint limit in this case.

To find the minimum set of actuated joints, the right-hand side of (32) is rewritten as

$$[\,B_o \quad \mathbf{a_3}\,] \begin{bmatrix} \dot{\phi}_f \\ \dot{\phi}_{oc} \\ \dot{\beta}_{oc} \\ \dot{\eta} \end{bmatrix} = [\,A \quad A_C\,] \begin{bmatrix} \mathbf{u_A} \\ \mathbf{u_C} \end{bmatrix}. \tag{33}$$

For simplification, let $l_{oc} = l_f = l$, $d_{oc} = d$, $r_f = r_{oc} = r$, and $\beta_{oc} = \beta$. Using A_C shown at the bottom of the previous page, $\mathbf{u_C}$ can be found to be the same as in Case 1. In this case, the minimum actuated joints set is either $\{\dot{\phi}_f, \dot{\beta}_{oc}, \dot{\eta}\}$ or $\{\dot{\phi}_{oc}, \dot{\beta}_{oc}, \dot{\eta}\}$.

3) Case 3: Base With Two Fixed Wheels + a Revolute Joint: Fig. 5 shows the case where two fixed wheels are attached to the base. The link is connected through a revolute joint to the base. The base motion ${}^{\mathbf{R}}\dot{\mathbf{p}}$ is constrained to

$$\begin{bmatrix} -1 & 0 & l_{f1}\cos\beta_{f1} \\ -1 & 0 & l_{f2}\cos\beta_{f2} \\ 0 & 1 & l_{f1}\sin\beta_{f1} \\ 0 & 1 & l_{f2}\sin\beta_{f2} \end{bmatrix} R^{-1}(\theta)\,{}^{\mathbf{R}}\dot{\mathbf{p}} + \begin{bmatrix} r_{f1} & 0 \\ 0 & r_{f2} \\ 0 & 0 \\ 0 & 0 \end{bmatrix} \begin{bmatrix} \dot{\phi}_{f1} \\ \dot{\phi}_{f2} \end{bmatrix} = \mathbf{0}. \tag{34}$$

Then ${}^{\mathbf{F}}\mathbf{v_E}$ is constrained to

$$\begin{bmatrix} -1 & 0 & l_{f1}\cos\beta_{f1} \\ -1 & 0 & l_{f2}\cos\beta_{f2} \\ 0 & 1 & l_{f1}\sin\beta_{f1} \\ 0 & 1 & l_{f2}\sin\beta_{f2} \end{bmatrix} {}^{\mathbf{F}}\mathbf{v_E} = \begin{bmatrix} -r_{f1} & 0 \\ 0 & -r_{f2} \\ 0 & 0 \\ 0 & 0 \end{bmatrix} \mathbf{a_3} \begin{bmatrix} \dot{\phi}_{f1} \\ \dot{\phi}_{f2} \\ \dot{\eta} \end{bmatrix}. \tag{35}$$

To meet the conditions of **Theorem 1**,

- $l_{f1}\sin\beta_{f1} = l_{f2}\sin\beta_{f2} \neq 0$;
- $l_{f1}^2 + l_{f2}^2 - 2l_{f1}l_{f2}\cos(\beta_1 - \beta_2) \neq 0$.

The first condition means that the wheels must share the same rotation axis and ${}^{\mathbf{r}}\mathbf{x_E}$ must not lie on this axis. The second condition implies that the ground contact points of the two wheels must not coincide. Since rank $B = 3$ (rank $A_C = 0$) in this case, all the three input variables, $\dot{\phi}_{f1}$, $\dot{\phi}_{f2}$, and $\dot{\eta}$ are required to steer the link motion in the omnidirectional manner. From this structure, the omnidirectional robot OmniKity-III has been developed. The robot structure is described in the next section with the kinematic model and its fault-tolerance property.

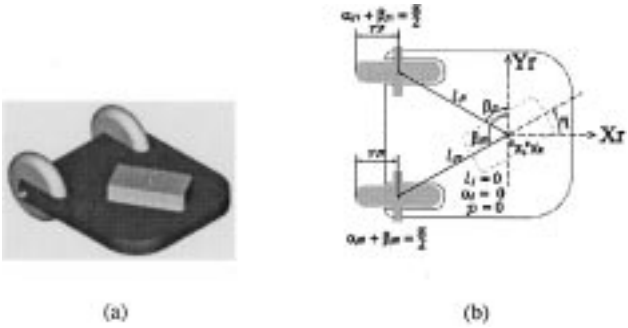

Fig. 5. Case 3. (a) 3-D view. (b) Kinematic parameters.

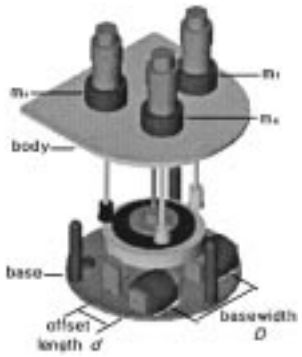

Fig. 6. Overall view of the mechanism (motor axes are exaggeratedly lengthened).

V. OmniKity-III

In Section IV, several cases were examined to produce omnidirectional motion using a conventional wheeled base with $\delta_m = 2$ and an extra prismatic or revolute joint. It was concluded that a revolute joint is more appropriate than a prismatic joint because a prismatic joint motion is restricted mechanically when it is fully expanded or shrunk, while a revolute joint can rotate unhindered in both directions. Amongst the examples, Case 3 was further improved to develop OmniKity robot series [6]. In addition to the differentially driven wheeled base with a revolute joint structure, a novel gear train was devised to have fault tolerance so that, in the event of failure in any one of the motors, the robot posture is still controllable with the other two motors.

A. Description of Mechanism

Fig. 6 shows the overall view of the mechanism. The robot consists of a differentially driven wheeled base and the rotating body. The three dc motors are mounted on the body. The base is supported by two fixed wheels and one castor wheel. The rotational motion of the motors is transmitted to the two fixed wheels on the base and the revolute joint through a novel gear train. The gear train helps to avoid the mechanical joint limitations on the revolute motion.

Fig. 7 shows the torque flow from each motor. The driving force of motor m_c produces $\dot{\eta}$, the rotational motion of the body with respect to the base, by exerting a force on $\mathbf{G_{fc}}$ which is fixed to the base. The rotating force of motor m_l is transmitted to the left base gear $\mathbf{G_{bl}}$ via the free rotating gear $\mathbf{G_{fl}}$, which has pinion gears on the side to be meshed with the motor gear $\mathbf{G_{ml}}$ and crown gears on the bottom to be meshed with $\mathbf{G_{bl}}$. Then the rotating motion of $\mathbf{G_{bl}}$ is transmitted

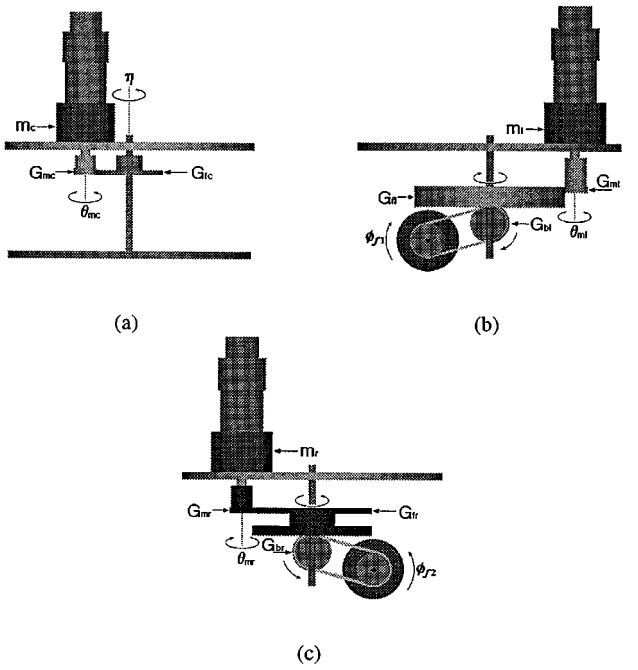

Fig. 7. Motion flow (a) from motor m_c to revolute joint, (b) from motor m_l to left wheel, and (c) from motor m_r to right wheel.

to the left wheel motion $\dot{\phi}_{f1}$ via a timing belt. In the same manner, the rotating force of motor m_r is transmitted to the right wheel motion $\dot{\phi}_{f2}$. Bearings are inserted between the two free rotating gears $\mathbf{G_{fl}}$ and $\mathbf{G_{fr}}$ to minimize friction or mechanical coupling between them. Since the motor m_c rotates the body where motors m_l and m_R are mounted, its motion contributes to $\dot{\phi}_{f1}$ and $\dot{\phi}_{f2}$ in the following manner:

$$\begin{bmatrix} \dot{\phi}_{f1} \\ \dot{\phi}_{f2} \end{bmatrix} = \begin{bmatrix} -\dfrac{N_{mc}}{N_{ic}}\dfrac{N_{il}}{N_{wl}} & 0 & \dfrac{N_{ml}}{N_{wl}} \\ \dfrac{N_{mc}}{N_{ic}}\dfrac{N_{ir}}{N_{wr}} & \dfrac{N_{mr}}{N_{wr}} & 0 \end{bmatrix} \begin{bmatrix} \dot{\theta}_{mc} \\ \dot{\theta}_{mr} \\ \dot{\theta}_{ml} \end{bmatrix} \tag{36}$$

where $\dot{\theta}_{mc}$, $\dot{\theta}_{mr}$, and $\dot{\theta}_{ml}$ are the center, the right, and the left motor rotating motion, respectively.

Table I lists kinematic parameters including the gears and their teeth values.

B. Kinematic Equations and Properties

From (35), ${}^{\mathbf{F}}\mathbf{v_E}$ is constrained to

$$\begin{bmatrix} -1 & 0 & \dfrac{D}{2} \\ -1 & 0 & -\dfrac{D}{2} \\ 0 & 1 & -d \\ 0 & 1 & -d \end{bmatrix} {}^{\mathbf{F}}\mathbf{v_E} = \begin{bmatrix} -r & 0 & \dfrac{D}{2} \\ 0 & -r & -\dfrac{D}{2} \\ 0 & 0 & -d \\ 0 & 0 & -d \end{bmatrix} \begin{bmatrix} \dot{\phi}_{f1} \\ \dot{\phi}_{f2} \\ \dot{\eta} \end{bmatrix} \tag{37}$$

or

$${}^{\mathbf{F}}\mathbf{v_E} = \begin{bmatrix} \dfrac{r}{2} & \dfrac{r}{2} & 0 \\ -\dfrac{dr}{D} & \dfrac{dr}{D} & 0 \\ -\dfrac{r}{D} & \dfrac{r}{D} & 1 \end{bmatrix} \begin{bmatrix} \dot{\phi}_{f1} \\ \dot{\phi}_{f2} \\ \dot{\eta} \end{bmatrix} \tag{38}$$

where $[\dot{\phi}_{f1}\ \dot{\phi}_{f2}\ \dot{\eta}]^T$ is represented by the gear train as

$$\begin{bmatrix} \dot{\phi}_{f1} \\ \dot{\phi}_{f2} \\ \dot{\eta} \end{bmatrix} = \begin{bmatrix} -\dfrac{N_{mc}}{N_{ic}}\dfrac{N_{il}}{N_{wl}} & 0 & \dfrac{N_{ml}}{N_{wl}} \\ \dfrac{N_{mc}}{N_{ic}}\dfrac{N_{ir}}{N_{wr}} & \dfrac{N_{mr}}{N_{wr}} & 0 \\ \dfrac{N_{mc}}{N_{ic}} & 0 & 0 \end{bmatrix} \begin{bmatrix} \dot{\theta}_{mc} \\ \dot{\theta}_{mr} \\ \dot{\theta}_{ml} \end{bmatrix}. \tag{39}$$

TABLE I
KINEMATIC PARAMETERS

Variable	Description	Values
d	offset length	4.2 cm
D	basewidth	9.2 cm
r	wheel radius	2.2 cm
N_{mc}	center motor gear ($\mathbf{G_{mc}}$) teeth	18
N_{mr}	right motor gear ($\mathbf{G_{mr}}$) teeth	18
N_{ml}	left motor gear ($\mathbf{G_{ml}}$) teeth	18
N_{ic}	center fixed gear ($\mathbf{G_{fc}}$, fixed to the base) teeth	94
N_{ir}	right free rotating gear ($\mathbf{G_{fr}}$) teeth	118
N_{il}	left free rotating gear ($\mathbf{G_{fl}}$) teeth	94
N_{wr}	right base gear ($\mathbf{G_{br}}$) teeth	30
N_{wl}	left base gear ($\mathbf{G_{bl}}$) teeth	30

TABLE II
ANGULAR VELOCITY COEFFICIENTS

Situation	a	b
$\dot{\theta}_{mc}$=0	1	0
$\dot{\theta}_{mr}$=0	$1+\frac{D}{2r}\frac{N_{mc}}{N_{mr}}\frac{N_{wr}}{N_{ir}}(\approx 1.532)$	$\frac{1}{r}\frac{N_{mc}}{N_{mr}}\frac{N_{wr}}{N_{ir}}(\approx 0.116)$
$\dot{\theta}_{ml}$=0	$1+\frac{D}{2r}\frac{N_{mc}}{N_{ml}}\frac{N_{wl}}{N_{il}}(\approx 1.667)$	$-\frac{1}{r}\frac{N_{mc}}{N_{ml}}\frac{N_{wl}}{N_{il}}(\approx -0.145)$

Denoting J_1 as the 3×3 matrix on the right-hand side of (38) and J_2 as that of (39), ${}^{\mathbf{F}}\mathbf{v_E}$ is represented as

$${}^{\mathbf{F}}\mathbf{v_E} = J_1 \cdot J_2 \cdot \begin{bmatrix} \dot{\theta}_{mc} \\ \dot{\theta}_{mr} \\ \dot{\theta}_{ml} \end{bmatrix}. \tag{40}$$

Then ${}^{\mathbf{R}}\dot{\mathbf{p}}_{\mathbf{E}}$, the body motion with respect to the global frame $\mathbf{\Sigma_R}$, is represented as

$${}^{\mathbf{R}}\dot{\mathbf{p}}_{\mathbf{E}} = R(\theta) \cdot {}^{\mathbf{F}}\mathbf{v_E} \tag{41}$$

$$= R(\theta) \cdot J_1 \cdot J_2 \cdot \begin{bmatrix} \dot{\theta}_{mc} \\ \dot{\theta}_{mr} \\ \dot{\theta}_{ml} \end{bmatrix} \tag{42}$$

with $\dot{\theta} = {}^{\mathbf{F}}v_{\theta E} - \dot{\eta} = \dot{\theta}_E - N_{mc}/N_{ic}\dot{\theta}_{mc}$.

Remark 4: Because of the nondiagonal terms of the 3×3 matrix in (39), the two wheel motions $\dot{\phi}_{f1}$ and $\dot{\phi}_{f2}$ are independently controllable even if any one of the motors fails, which is then assumed to be locked. This property, in turn, leads to the controllability of ${}^{\mathbf{R}}\mathbf{p_E}$ in such cases.

Property 1: The posture of OmniKity-III, ${}^{\mathbf{R}}\mathbf{p_E}$, is controllable even if any one of the three motors is locked from a failure.

Proof: If one of the motors is locked from a failure, the kinematic model assumes the following form:

$$\begin{bmatrix} {}^{\mathbf{R}}\dot{\mathbf{p}}_{\mathbf{E}} \\ \dot{\theta} \end{bmatrix} = \begin{bmatrix} \dot{x}_E \\ \dot{y}_E \\ \dot{\theta}_E \\ \dot{\theta} \end{bmatrix} = \begin{bmatrix} \cos\theta & -d\sin\theta \\ \sin\theta & d\cos\theta \\ b & a \\ 0 & 1 \end{bmatrix} \begin{bmatrix} v \\ \omega \end{bmatrix} \tag{43}$$

where

$$\begin{bmatrix} v \\ \omega \end{bmatrix} = \begin{bmatrix} \dfrac{r}{2} & \dfrac{r}{2} \\ -\dfrac{r}{d} & \dfrac{r}{d} \end{bmatrix} \begin{bmatrix} \dot{\phi}_{f1} \\ \dot{\phi}_{f2} \end{bmatrix} \tag{44}$$

and the constants a and b are as given in Table II. Using Chow's Theorem, the controllability of ${}^{\mathbf{R}}\mathbf{p_E}$ is shown in the following.

When $b = 0$, θ_E is represented as $\theta_E = a\cdot\theta + \text{constant}(a \neq 0)$. So, in order to prove the controllability of ${}^{\mathbf{R}}\mathbf{p_E} = [x_E\ y_E\ \theta_E]^T$, it is sufficient to prove the controllability of $[x_E\ y_E\ \theta]^T$. The motion equation of $[x_E\ y_E\ \theta]^T$ is given by

$$\begin{bmatrix} \dot{x}_E \\ \dot{y}_E \\ \dot{\theta} \end{bmatrix} = \begin{bmatrix} \cos\theta & -d\sin\theta \\ \sin\theta & d\cos\theta \\ 0 & 1 \end{bmatrix} \begin{bmatrix} v \\ \omega \end{bmatrix}. \tag{45}$$

Let $\mathbf{g_1}$, $\mathbf{g_2}$ be the columns of the 3×2 matrix on the right-hand side of (45), then

$$\mathrm{rank}[\ \mathbf{g_1} \quad \mathbf{g_2} \quad [\mathbf{g_1}, \mathbf{g_2}]\ ] = 3. \tag{46}$$

Hence the posture variables are controllable.

When $b \neq 0$, let $\mathbf{g_1}$ and $\mathbf{g_2}$ be the columns of the 4×2 matrix on the right-hand side of (43), then

$$\mathrm{rank}[\ \mathbf{g_1} \quad \mathbf{g_2} \quad [\mathbf{g_1}, \mathbf{g_2}] \quad [\mathbf{g_2}, [\mathbf{g_1}, \mathbf{g_2}]]\ ] = 4. \tag{47}$$

Thus, ${}^{\mathrm{R}}\mathbf{p_E}$ is controllable. □

The control laws in actuator failure are proposed and demonstrated in [6].

VI. Conclusion

In this paper, the mobility augmentation method was proposed to produce omnidirectional motion with conventional wheeled bases with the degree of mobility less than three. Combined with a revolute/prismatic joint, some conventional wheeled bases with the degree of mobility less than three could produce omnidirectional motion if some conditions were satisfied. The structural conditions for mobility augmentation were derived and several examples were provided. Such a nonconventional omnidirectional mechanism did not suffer from typical problems that conventional omnidirectional mechanisms have.

One of the illustrated structures was further improved to develop the OmniKity robot series. A novel gear train was devised so that, in addition to the omnidirectional property, the mechanism provides a fault-tolerance property in case of the failure of any one of the three motors.

References

[1] G. Campion, G. Bastin, and B. D'Andrea-Novel, "Structural properties and classification of kinematic and dynamic models of wheeled mobile robots," *IEEE Trans. Robot. Automat.*, vol. 12, pp. 47–62, 1996.

[2] S. L. Dickerson, "Control of an omni-directional robotic vehicle with mecanum wheels," in *National Telesystems Conf.*, 1991, pp. 323–328.

[3] L. Ferriere and B. Raucent, "ROLLMOBS, a new universal wheel concept," in *IEEE Int. Conf. on Robotics and Automation*, 1998, pp. 1877–1882.

[4] R. Holmberg and O. Khatib, "Development and control of a holonomic mobile robot for mobile manipulation tasks," *Int. J. Robot. Res.*, vol. 19, no. 11, pp. 1066–1074, 2000.

[5] M.-J. Jung, H.-S. Shim, H.-S. Kim, and J.-H. Kim, "The miniature omnidirectional mobile robot OmniKity-I (OK-I)," in *IEEE Int. Conf. on Robotics and Automation*, 1999, pp. 2686–2691.

[6] M.-J. Jung and J.-H. Kim, "Fault tolerant control strategy of OmniKity-III," in *IEEE Int. Conf. on Robotics and Automation*, 2001, pp. 3370–3375.

[7] S. M. Killough and F. G. Pin, "Design of an omnidirectional and holonomic wheeled platform prototype," in *IEEE Int. Conf. on Robotics and Automation*, 1992, pp. 84–90.

[8] P. F. Muir and C. P. Neuman, "Kinematic modeling for feedback control of an omnidirectional wheeled mobile robot," in *IEEE Int. Conf. on Robotics and Automation*, 1987, pp. 1772–1778.

[9] M. Wada and S. Mori, "Holonomic and omnidirectional vehicle with conventional tires," in *IEEE Int. Conf. on Robotics and Automation*, 1996, pp. 3671–3676.

[10] M. West and H. H. Asada, "Design and control of ball wheel omnidirectional vehicles," in *IEEE Int. Conf. on Robotics and Automation*, 1995, pp. 1931–1938.

[11] B. Yi and W. K. Kim, "The kinematics for redundantly actuated omni-directional mobile robots," in *IEEE Int. Conf. on Robotics and Automation*, 2000, pp. 2485–2492.

Optimal Mobile Robot Pose Estimation Using Geometrical Maps

Geovany Araujo Borges and Marie-José Aldon

***Abstract*—We propose a weighted least-squares (WLS) algorithm for optimal pose estimation of mobile robots using geometrical maps as environment models. Pose estimation is achieved from feature correspondences in a nonlinear framework without linearization. The proposed WLS approach yields optimal estimates in the least-squares sense, is applicable to heterogeneous geometrical features decomposed in points and lines, and has an $O(N)$ computation time.**

***Index Terms*—Heterogeneous features, nonlinear optimization, optimal 2-D pose estimation, weighted least-squares.**

I. Introduction

In mobile robot absolute localization, depending on the employed approach, we encounter the problem of estimating the 2-D transformation parameters (rotation and translation) that relate two sets of geometrical features extracted from two different maps. In the context of absolute localization, we have a global map $\mathcal{M}$, which may be continuously updated, and a local map $\mathcal{M}'$ which is composed of geometrical features extracted from exteroceptive sensor readings such as a video camera [1], a laser rangefinder [2], ultrasonic ranging [3], [4], or a combination of them [5]. Usually, maps are composed of heterogeneous geometrical features such as points, which correspond to corners and vertical edges in the environment, and lines which represent walls and sides of polygonal obstacles. Map building using different types of features allows a greater reliability for the pose estimation.

Most of the proposed methods which use geometrical features for map-based pose estimation are divided into three phases: pose prediction, feature matching between maps $\mathcal{M}$ and $\mathcal{M}'$, and pose estimation from the matched features. Pose prediction provides an initial guess of the vehicle's pose and an associated uncertainty measure, which are used as prior information for feature matching between $\mathcal{M}$ and $\mathcal{M}'$. From the feature correspondences, the estimation phase provides a pose estimate and an associated uncertainty measure which optimize some criterion. The work presented in this paper only concerns the pose estimation phase.

II. Background

The most used approach for map-based mobile robot pose estimation using geometrical features is the extended Kalman filter (EKF) [6], [7]. The formulation of the mobile robot localization problem using the EKF is elegant and allows one to fuse multisensory data. The problem is generally written as that of estimating the state of a discrete stochastic nonlinear dynamic system which evolves using proprioceptive sensor readings u as

$$z(k) = g(z(k-1), u(k)) + v(k) \tag{1}$$

with v modeling a Gaussian noise with distribution $N(\mathbf{0}, \boldsymbol{P}_v(k))$ (multivariate normal distribution with zero mean and covariance $\boldsymbol{P}_v(k)$).

Manuscript received February 14, 2001; revised November 7, 2001. This paper was recommended for publication by Associate Editor M. Buehler and Editor S. Hutchinson upon evaluation of the reviewers' comments. This work was supported in part by Capes, Brasília, Brazil, under Grant BEX2280/97-3

The authors are with the Robotics Department, Laboratoire d'Informatique, de Robotique et de Microélectronique de Montpellier, UMR CNRS/UM2, C55060 Montpellier, France (e-mail: borges@lirmm.fr; aldon@lirmm.fr).

Publisher Item Identifier S 1042-296X(02)01775-5.